Theoretical Investigation of The Properties of LiRuAs Semi-Heusler Alloy via Density Function Theory

Erol ALBAYRAK[1*]

[1]*Kırşehir Ahi Evran University, Faculty of Engineering and Architecturte, Department of Metallurgy and Material Engineering, Kırşehir, Turkey*
ORCID: 0000-0001-9161-9068

Abstract

The structural, thermal, electronic and elastic properties of LiRuAS Semi Heusler alloy were investigated using a generalized gradient approximation (GGA) approach, which employs a density functional theory (DFT) to examine the alloy's optimized equilibrium lattice parameter. The optimized lattice parameter was found to be 5.601 Å. The results of the calculations indicate that the alloy was mechanically stable. Additionally, owing to the modulus and certain ratios, such as the bulk modulus Young's modulus the alloy was found to have low compressibility and a soft, ductile and anisotropic natüre. The Debye temperature of the alloy was calculated to be 281.186 K. We believe that the LiRuAs SH alloy may be particularly useful for magnetic field shielding applications due to its metallic conductive and nonmagnetic nature.

1. Introduction

Technology has become one of the almost indispensable facts in our lives in the 21st century. With the development of technology, people's quality and duration of life have increased. Materials science has played a major role in the development of technology. New applications of elements and materials composed of these elements, especially in the field of electronics, have enabled technology to advance step by step daily. As new generation smart materials, nanomaterials, semiconductors, and magnetic and nonmagnetic materials are examined, their previously unknown properties are determined, and new comfort areas are offered to humanity thanks to devices made using these properties.

In a 1903 study, it was observed that the alloys examined could have magnetic properties, although the elements that make up the alloys obtained were not magnetic [1]. This showed that some properties that are not present in the constituent elements of the alloys may be present in the alloys from which they are synthesized. Based on the abovementioned work, such alloys have been given the general name Heusler alloys, and these alloys

have been studied, especially for the production of new generation magnetoelectronic and spintronic devices. Heusler alloys generally consist of four nested face-centered cubic (FCC) cells, and their general formula was initially determined to be $XY_2 Z$. Studies have shown that one of these FCC cells can be removed from alloys and that the properties of the new alloy formed in this way can change compared to those in the initial state. In this way, the alloys obtained by removing a subcell from the alloys in accordance with the general formula $XY_2 Z$ are called Semi-Heusler (SH) alloys. The general formula for preparing Semi-Heusler alloys is XYZ [2]. Heusler alloys are generally costly and time consuming to obtain. It is also possible that not all synthesized alloys are promising for various applications [3 -11]. Therefore, it is logical and scientific to determine promising materials by performing theoretical studies before the experimental study of alloys and to proceed to the device production stage by performing experimental studies after this stage.

In this study, the electronic, structural, elastic, thermal and physical properties of LiRuAs SH alloys were investigated with the help of the Quantum-

---

ESPRESSO software package, which includes a density function theory (DFT) approach [12,13].

2. Material and Method

The state in which a material has minimum energy is called steady-state energy. The lattice constant of the material at this minimum energy is called the steady-state lattice constant. These constants are used to determine many properties of the material. To determine the steady-state lattice constants of materials, it is necessary to know the interactions between the electrons and atoms in the material. In this study, the DFT approach was used to theoretically calculate the steady-state optimized lattice constant and structural, electronic, and thermal properties of the material. To perform calculations with this approach, the ground-state electronic charge density expression proposed by Kohn and Sham in 1965 was used [14].

To perform calculations for the minimum-energy steady state, it is necessary to determine the exchange correlation potential of noninteracting electrons. This potential is determined by an approach called the local density approximation (LDA) [15]. To improve the success rate of the calculations, a group of scientists developed the Perdew-Burke-Ernzehof generalized gradient approximation (PBE-GGA) [16] The PBE-GYY approach was also used for the calculations performed in this study for the LiRuAs SH alloy. In addition to these approaches, it is necessary to solve the Schrödinger Equation in equation 1 to calculate the minimum energy of the alloy.

$$H\varphi = \varepsilon\varphi \qquad (1)$$

To solve this equation, potential contributions from the cor and valence electrons must be added to the equation. In the calculations, Rappe group potentials were selected from the potential pseudo potentials required for the LiRuAs SH alloy [17]. In the calculations, the plane wave shear energy was chosen as 40 Ry, the electronic charge density was chosen as 400 Ry, and the integration k-points in the Brilloin region were chosen as 8x8x8. The smearing parameter up to the Fermi surface was set as 0.02 Ry, and the Methfessel-Paxton smearing technique was used for the calculations [18]. Calculations for the thermodynamic and elastic properties of the alloy were performed with the Thermo_pw program using the Debye model [19].

3. Results and discussion

3.1. Structural features

The atoms of the LiRuAs SH alloy have an atomic arrangement belonging to the F$\bar{4}$3 m space group. Since the alloy has a SH structure, it has the general formula XYZ. Atomic positions of the unit cell of the alloy: (0, 0, 0, 0) for As atoms, (1/4, 1/4, 1/4, 1/4) for Li atoms and (3/4, 3/4, 3/4, 3/4) for Ru atoms. Figure 1 shows the unit cell structure of the F$\bar{4}$3 m crystalline LiRuAs SH alloy by using the Vesta programme.
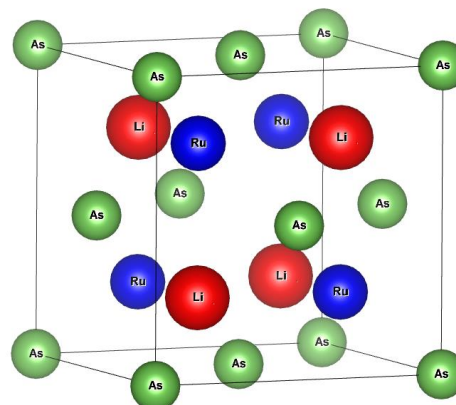

Figure 1. Unit cell structure of LiRuAs SH alloy with F$\bar{4}$3 m crystal arrangement.

A literature search on LiRuAs SH alloy revealed that there are no experimental studies on the alloy. To test the reliability of the results of the calculations for the alloy, models for the possible steady states of the alloy were created on the Open Quantum Materials Database [20] website. All three different atomic arrangements of the alloy are in the F$\bar{4}$3 m space group. Calculations were made for the alloy with these three different atomic arrangements, and it was determined that the lowest energy state could be the most stable state. All calculations were performed based on the unit cell structure of this alloy, as shown in Figure 1.

The optimized equilibrium state lattice constant was calculated with the Quantum Espresso program, where the total energy was a minimum of $a_0 = 5,601$ Å. This value is only 0.176% different from the lattice constant value reported on The Open Quantum Materials Database website, and the reliability of the calculations was confirmed by the agreement between the calculations and the values on the website.

3.2. Electronic specifications

To understand the electronic and magnetic properties of a material, elastic constants must be calculated, and

electronic band curves must be plotted along the spin-up and spin-down axes. In addition, density of states (DOS) plots are plotted to better understand the contribution of the atoms in the alloy to the conductivity. Figure 2 shows the electronic band curves obtained from calculations to understand the electronic and magnetic properties of the LiRuAs SH alloy.
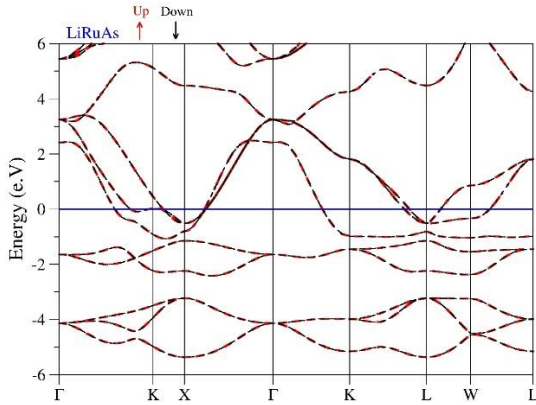

Figure 2. Electronic band graph of LiRuAs SH alloy.

According to the graph, the high symmetry axes in the valence and conduction bands overlap in the spin-up ($\uparrow$) and spin-down ($\downarrow$) directions, and the curves in the conduction band cross the Fermi energy level. The fact that the curves cross the Fermi energy level helps us to understand that there is no forbidden energy gap between the valence and conduction bands; therefore, electrons can be exchanged between both bands. This means that there is no forbidden energy gap near the Fermi energy level, and therefore, the alloy is a metallic conductor.

In addition, the fact that the curves coincide on the spin-up and spin-down high-symmetry axes allows us to understand that the alloy has a nonmagnetic character, that is, the magnetic moment is zero. Partial and total density of states (DOS) curves of the alloy were plotted, and the plotted curves are shown in Figure 3.
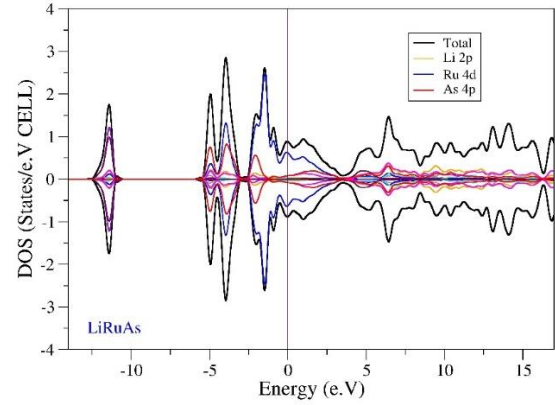

Figure 3. Density of state (DOS) plot of LiRuAs SH alloy.

According to the graph of the alloy, the most dominant contribution to the electrical conductivity in the spin-up and spin-down high symmetry orientations comes from the 4d, 2p and 4p orbitals of Ru, Li, As and Fe, respectively. The contributions of the other elements in the alloy to the electronic conductivity were found to be quite limited. The fact that the DOS curves are symmetric allows us to understand that the alloy does not have a magnetic moment [21].

3.3. Elastic properties

To understand the elastic properties of a material, several moduli and ratios, such as the bulk modulus (*B*), Young's modulus (*E*), shear modulus (*G*), and B/G ratio, should be calculated.

To make these calculations, it is necessary to calculate the values of C_{11}, C_{12} and C_{44}, which are called elastic constants. By using elastic constants, we can also understand whether the material is mechanically stable according to the Born criteria. For the material to be mechanically stable, the elastic constants must meet the Born stability criteria given in Equation 2 [22].

$$C_{44} > 0; \ C_{11} - C_{12} > 0; \ C_{11} + 2C_{12} > 0 \qquad (2)$$

Using the obtained elastic constants, the moduli and ratios are calculated to understand certain properties, such as the hardness, softness and brittleness of the material. Table 1 shows the elastic constants obtained from the calculations for the LiRuAs SH alloy.

Table 1. Calculated elastic constants for LiRuAs SH alloy (C_{11}, C_{12} and C_{44}; GPa)

Material	C_{11}	C_{12}	C_{44}
LiRuAs	148.425	96.515	30.187

The equations that allow us to calculate the moduli and ratios that help us understand some of the elastic and physical properties of the alloy are given below. All moduli and ratios given in Table 2 were obtained using these equations [23].

$$A = \frac{2C_{44}}{C_{11} - C_{12}} \quad (3)$$

$$\sigma = \frac{1}{2}(1 - \frac{E}{3B}) \quad (4)$$

$$B = \frac{2C_{12} + C_{11}}{3} \quad (5)$$

$$E = \frac{9BG}{3B + G} \quad (6)$$

$$G = \frac{5(C_{11} - 2C_{12})C_{44}}{3(C_{11} - 2C_{12}) + C_{44}} \quad (7)$$

Table 2. Bulk modulus (*B*; GPa), shear modulus (*G*; GPa), Young's modulus (*E*; GPa), *B/G* ratio, Poisson's ratio (σ), and anisotropy factor (*A*) were calculated for the LiRuAs SH alloy.

Material	*B*	*G*	*E*	*B/G*	σ	*A*
LiRuAs	113.8	28.4	78.7	4.01	0.385	1.16

The Alloy $C_{11} - C_{12}$ difference is positive. This difference between the elastic constants is called Cauchy Pressure. A positive Cauchy pressure allows us to understand that the bonds in the alloy are significantly ionic. In addition, a Poisson's ratio of approximately 0.25 indicates that the bonds in the alloy are significantly ionic [24]. The bulk moduli calculated for the alloys are given in Table 2 $C_{12} <$

$B < C_{11}$ and were calculated in the range of 100 GPa. A bulk modulus greater than 100 GPa indicates that the alloy has low compressibility. The larger the Young's modulus is, the greater the hardness of the material.

The Young's modulus calculated for the LiRuAs SH alloy is less than 100 GPa, and accordingly, the alloy is considered to be soft.

According to Pugh's criterion, the *B/G* ratio provides information about the ductile or brittle nature of materials. If the *B/G* ratio is greater than 1.75, the material is considered ductile, and if it is smaller, it is considered brittle. The calculated *B/G* ratio of 4.007 for the LiRuAs SH alloy allows us to understand that the alloy has a ductile nature [25].

Anisotropy can be explained as the directional dependence of some properties of a material during forming. The calculated anisotropy for the LiRuAs SH alloy is very slightly different from 1. Since the anisotropy factor is different from 1, we were able to infer that the alloy is anisotropic; that is, some physical properties of the alloy may change depending on the forming. Nevertheless, we believe that the fact that the anisotropy factor is very close to 1 may limit the effect of forming on the physical properties of the alloy during forming. The direction dependence of the Young's modulus, shear/shear modulus, Poisson's ratio and linear compressibility were calculated using ELATE codes, and their three-dimensional representations are given in Figures 4, 5 and 6 [26].
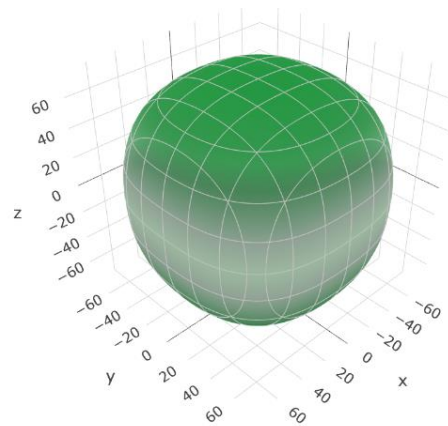

Figure 4. Three dimensional representation of the direction dependence of Young's modulus of LiRuAs SH alloy obtained with the help of Elate codes.
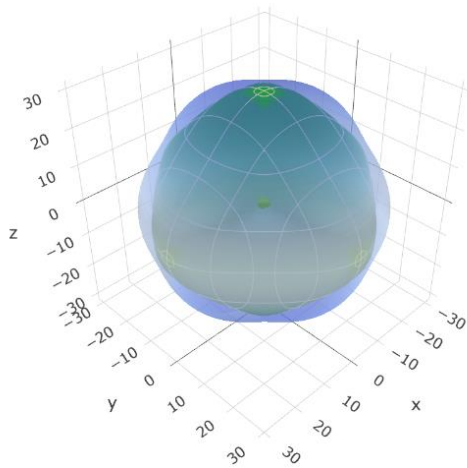
Figure 5. Three dimensional representation of the direction dependence of the shear modulus of LiRuAs SH alloy obtained with the help of Elate codes.
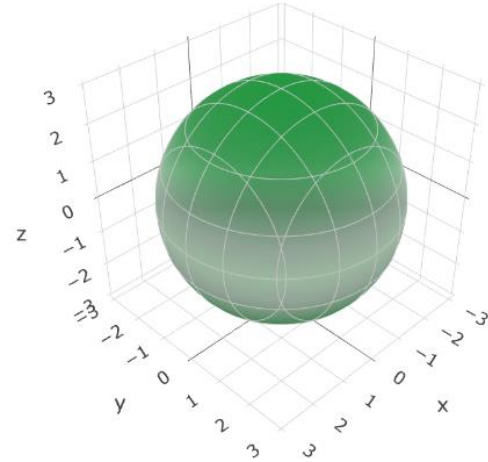

Figure 7. Three dimensional representation of the direction dependence of the linear compressibility of LiRuAs SH alloy obtained using Elate codes.
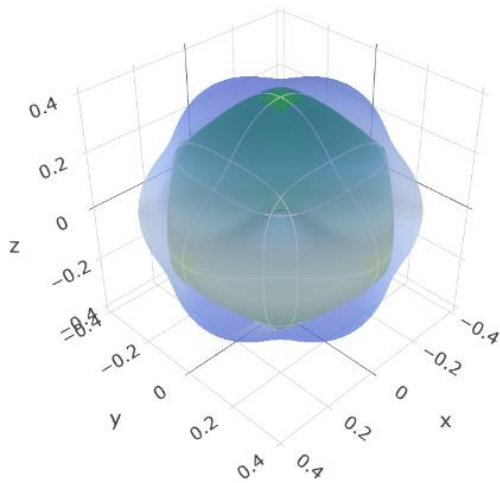

Figure 6. Three dimensional representation of the direction dependence of the Poisson's ratio of LiRuAs SH alloy obtained with Elate codes.

3.4. Thermal Properties

The thermal properties of the LiRuA SH alloy were investigated with the Thermo Pw program. The Thermo Pw program is based on the Debye model in its calculations. To understand the thermal properties of the alloy, the vibration energy-temperature, free vibration energy-temperature, heat capacity-temperature and entropy-temperature curves of the alloy were plotted. The plots are given in Figures 8, 9, 10 and 11.
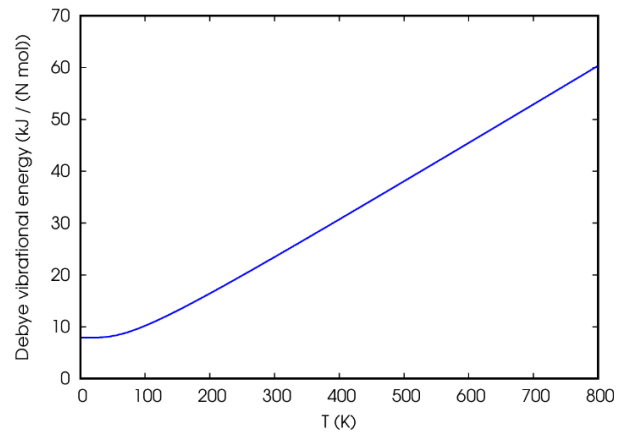

Figure 8. Vibration energy - Temperature plot of LiRuAs SH alloy

The internal energy of solid materials that receive heat increases. Increased internal energy is expected to increase the vibration of atoms in the material. In other words, the internal energy of a

material whose temperature increases; therefore, the vibration energy also increases. The correlation between temperature and vibration energy is shown in Figure 8. An increase in the temperature of a solid material leads to an increase in its internal energy, and an increase in internal energy leads to an increase in the vibration energy of the material. An increase in the vibrational energy of a material leads to a decrease in its free vibrational energy. Figure 9 shows the free vibration energy-temperature graph of the LiRuAs SH alloy. The graph shows that the free vibration energy decreases with temperature, as mentioned above.
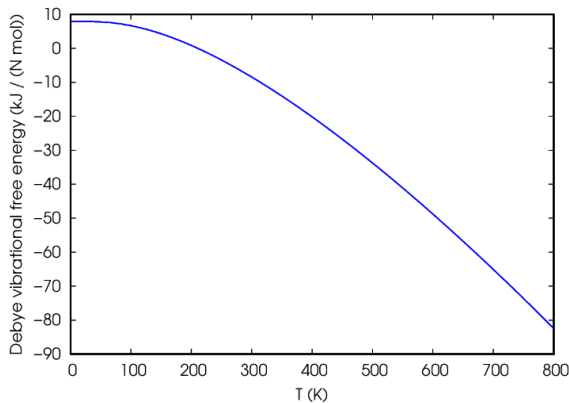

Figure 9. Free vibration energy - Temperature graph

The heat capacity-temperature graph in Figure 10 shows that the heat capacity of the alloy increases up to a certain temperature limit and then remains constant. This limit reached by the heat capacity of the LiRuA alloy is the Dulong-Petit limit [27]. The heat capacity of the alloy reached 3NR limit values with increasing temperature, confirming our expectation.
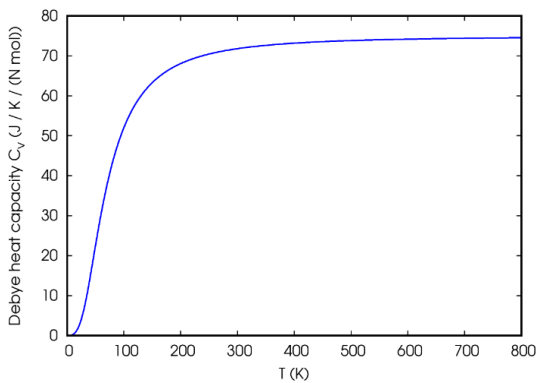

Figure 10. Heat capacity - temperature graph

As the temperature increases, the internal energy and atomic vibrations in the material also increase. This allows us to understand that the disorder in the material, i.e., the entropy, also increases with increasing temperature. Figure 11 shows the temperature-dependent graph of entropy. As expected, this graph shows that the disorder/entropy of a substance increases with temperature. The Debye temperature, which is a measure of the melting temperature of the alloy, was calculated to be 281.186 K.
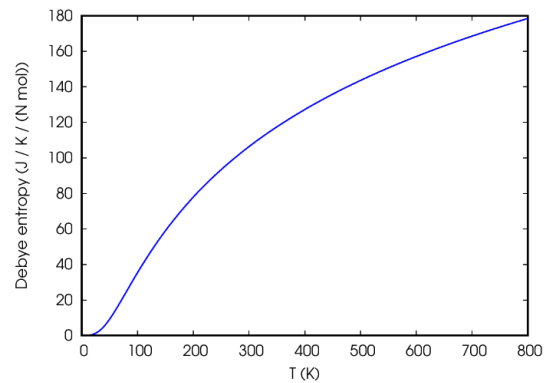

Figure 11. Entropy-temperature graph

4. Conclusion and Suggestions

In this study, several properties of LiRuAs SH alloys with F$\bar{4}$3 m space atomic arrangements were investigated theoretically using DFT. A literature search revealed that no experimental study of the alloy has been reported. Since Heusler alloys are both difficult and costly to obtain, it is important to determine theoretically the promising materials in areas such as spintronics and magnetoelectronic applications before experimental studies. The calculations for the alloy were performed with the Quantum Espresso program using the DFT approach.

The steady-state lattice constant of the alloy is $a_0 = 5,601$ Å. The value of 5,601 Å is in 99.824% agreement with the lattice constant calculated for the LiRuAs SH alloy on The Open Quantum Materials Database website. To understand the electronic properties of the alloy, electronic band curves and total and partial density of states (DOS) curves were plotted.

According to the information provided by these curves, the alloy has a net magnetic moment of zero and has a metallic conductive character. The calculation of the elastic constants of the alloy allowed us to make predictions about some of its

structural and physical properties. When the elastic constants were substituted for the Born stability criterion, we realized that the alloy was mechanically stable. Additionally, owing to the modulus and certain ratios, such as the bulk modulus Young's modulus the alloy was found to have low compressibility and a soft, ductile and anisotropic nature. The Poisson's ratio also showed that the atomic bonding in the alloy is largely ionic bonding.

To understand the thermal properties of the alloy, calculations were made in the Thermo Pw program using the Debye model, and the variations in the vibration energy, free vibration energy, heat capacity and entropy values of the alloy with temperature were examined. The Debye temperature of the alloy was calculated to be 281.186 K. We

believe that the LiRuAs SH alloy may be particularly useful for magnetic field shielding applications due to its metallic conductive and nonmagnetic nature. Although it is not desirable for the alloy to have zero magnetic moment for spintronic devices, it is thought that it can be used in applications that need magnetic isolation.

Conflict of Interest Statement

There is no conflict of interest between the authors.

Statement of Research and Publication Ethics

The study is complied with research and publication ethi

References

[1] R. F. Heusler, "Über Magnetische Manganlegierungen," *J. Verhandlungen der Deutschen Physikalischen Gesellschaft*, vol. 5, p. 219, 1903.

[2] G. Joseph Poon, "Chapter 2 Electronic and thermoelectric properties of Half-Heusler alloys," *Semiconductors and Semimetals*, vol. 70, pp. 37–75, 2001.

[3] S. Berri, D. Maouche, M. Ibrir, B. Bakri, "Electronic structure and magnetic properties of the perovskite cerium manganese oxide from ab initio calculations," *Materials Science in Semiconductor Processing*, vol. 26, pp. 199-204, 2014.

[4] F. Hosseinzadeh, A. Boochani, S.M. Elahi, Z. Ghorannevis, "GdPtBi Heuslerene: mechanical stability, half-metallic, magneto-optic, and thermoelectric properties by DFT", *Phil. Mag.*, vol. 102, p. 887–901, 2022.

[5] Y. Sokolovskaya, O. Miroshkina, D. Baigutlin, V. Sokolovskiy, M. Zagrebin, V. Buchelnikov, A.T. Zayak, "A ternary map of Ni–Mn–Ga Heusler alloys from ab initio calculations", *J. Met.*, vol. 11, p. 973, 2021.

[6] M. Çanlı, E. Ilhan, N. Arıkan, "First-principles calculations to investigate the structural, electronic, elastic, vibrational and thermodynamic properties of the full Heusler alloys X2ScGa (X= Ir and Rh) ", *J. Mater. Today Commun.*, vol. 26, p. 101855, 2021.

[7] J. Atulasimha, S. Bandyopadhyay, *Nanomagnetic and spintronic devices for energy-efficient memory and computing*, John Wiley & Sons. 2016.

[8] A. Bsiesy, "Spin injection into semiconductors: towards a semiconductor-based spintronic device", *J. Comptes Rendus Physique,* vol. 6, pp. 1022–1026, 2005.

[9] R.A.P. Ribeiro, A. Camilo, S.R. de Lazaro, "Electronic structure and magnetism of new ilmenite compounds for spintronic devices: FeBO3 (B= Ti, Hf, Zr, Si, Ge, Sn) ", *J. Magnet. Magnet. Mater.* Vol. 394 pp. 463–469, 2015.

[10]   Z. Chen, T. Li, T. Yang, H. Xu, R. Khenata, Y. Gao, X. Wang, " Palladium (III) fluoride bulk and PdF3/Ga2O3/PdF3 magnetic tunnel junction: multiple spin-gapless semiconducting, perfect spin filtering, and high tunnel magnetoresistance", *J. Nanomater.* Vol. 9, p. 1342, 2019.

[11]   J. M. Al-Issawe, I. Oreibi, " DFT Calculations of Trilayer Heterostructures from MoSe2, PtS2 Monolayers in Different Orders with Promising Optoelectronic Properties", *J.of the Turkish Chemical Society A*, vol. 11, pp. 405-414. 2024.

[12]   P. Gianozzi, S. Gironcoli, P. Pavone, S. Baroni, "Quantum Espresso: a modular and open-source software project for quantum simulations of materials," *Journal of Physics: Condensed Matter*, vol. 21, no. 39, p. 395502, 2009.

[13]   P. Giannozzi, O. Andreussi, T. Brumme, O. Bunau, M. B. Nardelli, M. Calandra, R. Car, C. Cavazzoni, D. Ceresoli, M. Cococcioni, N. Colonna, I. Carnimeo, A. D. Corso, S. de Gironcoli, P. Delugas, R. A. DiStasio Jr, A. Ferretti, A. Floris, G. Fratesi, G. Fugallo, R. Gebauer, U. Gerstmann, F. Giustino, T. Gorni, J. Jia, M. Kawamura, H-Y Ko, A. Kokalj, E. Küçükbenli, M. Lazzeri, M. Marsili, N. Marzari, F. Mauri, N. L. Nguyen, H-V Nguyen, A. Otero-de-la-Roza, L. Paulatto, S. Poncé, D. Rocca, R. Sabatini, B. Santra, M. Schlipf, A. P. Seitsonen, A. Smogunov, I. Timrov, T. Thonhauser, P. Umari, N. Vast, X. Wu and S. Baroni, "Advanced capabilities for materials modelling with QUANTUM ESPRESSO." *Journal of Physics: Condensed Matter,* vol 29, no 46, p. 465901, 2017.

[14]   L. J. Sham, W. Kohn, "Self-consistent equations including exchange and correlation effects," *Phys. Rev.*, vol. 140, p. A1133, 1965.

[15]   P. Gianozzi, P. Pavone, S. Baroni, "Ab initio calculation of phonon dispersions in semiconductors," *Phys. Rev. B*, vol. 43, no. 9, pp. 7231–7243, 1991.

[16]   J.P. Perdew, K Burke., M. Ernzerhof, "Generalized Gradient Approximation Made Simple," *Phys. Rev. Lett.*, vol. 77, no. 18, pp. 3865–3868, 1996.

[17]   G. P. Srivastava, *The physics of phonons*. Bristol.: Adam Hilger, 1990.

[17]   P. A. Methfessel M., "High-precision sampling for Brillouin- zone integration in metals," *Phys. Rev. B,* vol. 40, no. 6, p. 3616, 1989.

[19]   A. D. Corso, "Elastic constants of beryllium: a first-principles investigation," *J. Phys: Condens Matter*, vol. 28, no. 7, p. 075401, 2016.

[20]   "The Open Quantum Materials Database," *https://oqmd.org/.* [Online]. Available: https:// https://oqmd.org/materials/composition/LiRuAs

[21]   E. Albayrak., "XA yapıdaki Ti2RuSn ters-Heusler alaşımının yapısalı elektronik, elastik ve termodinamik özelliklerinin teorik olarak incelenmesi," *Journal of the Institute of Science and Technology*, vol. 12, no. 3, pp. 1496–1505, 2022.

[22]   K. Huang, M. Born, *Dynamical Teory of Crystal Lattices*. Oxford, England: Clarendon Press, 1965.

[23]   S. Al, N. Arikan, S. Demir and A. İyigor, "LatticeDynamic Properties of Rh2XAl (X= Fe and Y) Alloys," *Physica B: Condensed Matter*, vol. 531, pp. 16–20, 2018.

[24] V.V. Bannikov, I.R. Shein, A.L. Ivanovskii, "Electronic structure, chemical bonding and elastic properties of the first thorium-containing nitride perovskite TaThN3," *Physica status solidi (RRL) – Rapid Res. Lett.*, vol. 1, no. 3, pp. 89–91, 2007

[25] S. F. Pugh, *XCII. Relations between the elastic moduli and the plastic properties of polycrystalline pure metals*. London: The London, Edinburgh, and Dublin Philosophical Magazine and Journal of Science, 1954.

[26] R. Gaillac, P. Pullumbi, FX Coudert, "ELATE: an open-source online application for analysis and visualization of elastic tensors," *J. Phys.:Condens. Matter*, vol. 28, no. 27, p. 275201, 2016.

[27] P. Petit, "Recherches sur quelques points importants de la Théorie de la Chaleur," *Annales de Chimie et de Physique*, vol. 10395, p. 413, 1819.